Aragonite in olivine from Calatrava, Spain—Evidence for mantle carbonatite melts from >100 km depth

Emma R. Humphreys[1,2], Ken Bailey[1], Chris J. Hawkesworth[1,3], Frances Wall[4,2], Jens Najorka[2], and Andrew H. Rankin[5]
[1]Department of Earth Sciences, University of Bristol, Wills Memorial Building, Bristol BS8 1RJ, UK
[2]Department of Mineralogy, Natural History Museum, Cromwell Road, London SW7 5BD, UK
[3]University of St Andrews, College Gate, North Street, St Andrews, Fife KY16 9AJ, UK
[4]Camborne School of Mines, University of Exeter, Cornwall Campus, Penryn, Cornwall TR10 9EZ, UK
[5]School of Geography, Geology and the Environment, Kingston University, Surrey KT1 2EE, UK

ABSTRACT

Aragonite, as an inclusion in olivine from a leucitite lava flow, provides evidence for high-pressure crystallization and carbonatitic activity beneath the geophysical lithosphere in Calatrava, Spain. The aragonite occurs as a single crystal within olivine (Fo_{87}), interpreted to have crystallized from a carbonated silicate melt at mantle depths. Experimental data constrain the stability of aragonite to depths of >100 km at CO_2-H_2O-bearing mantle solidus temperatures. This is the first documented evidence of magmatic aragonite crystallized in the mantle. Entrained as xenocrysts, the olivines have not crystallized from the carrier melts, which must have formed deeper within the mantle. Lead isotope data of the leucitite and carbonate inclusions indicate that the source melts show isotopic enrichment relative to mid-oceanic ridge basalt and most ocean island basalt. Our evidence strengthens the argument for direct and deep mantle-derived volcanic carbonatite in alkaline volcanic provinces containing maar-type volcanism, such as Calatrava.

INTRODUCTION

In 2005, only 50 occurrences of carbonatite volcanism had been documented (Woolley and Church, 2005). The only currently active carbonatite volcano is Oldoinyo Lengai, Tanzania (Dawson, 1962), which erupts natrocarbonatite, a composition unlike anything else in the geological record (Woolley and Kempe, 1989; Bailey, 1993; Woolley and Church, 2005). Other examples of volcanic carbonatites include calcite carbonatite from a lapilli tuff at Kaiserstuhl, Germany (Keller, 1981), calcite carbonatite lava at Fort Portal, Uganda (Barker and Nixon, 1989), and dolomite carbonatite from Rufunsa, Zambia (Bailey, 1989). However, we anticipate from field observations in Europe and Africa that the number of carbonatitic volcanoes may increase to >300 examples.

A high-pressure mantle origin for many volcanic carbonatites is indicated by the presence of mantle xenoliths and other high-pressure and mantle-derived mineral phases, such as dolomite and magnesite (Bailey, 1989; Bailey et al., 2006), chromite (Bailey, 1989; Woolley et al., 1991) and high-Ti phlogopite (Bailey and Collier, 2000). Isotopic evidence from carbonatites is also indicative of a mantle origin (Deines and Gold, 1973; Bell and Simonetti, 2010).

Evidence for carbonatitic fluids at mantle temperatures and pressures includes the metasomatic effects documented from mantle xenoliths (e.g., Rudnick et al., 1993; Yaxley et al., 1998; Coltorti et al., 1999), the occurrence of carbonate minerals in mantle xenoliths (Rosatelli et al., 2007, and references therein), and high-pressure experimental results confirming the stability of carbonates and carbonatitic melts (Wyllie, 1978, and references therein). Inclusions within diamonds further demonstrate the activity of carbonate in the deep mantle (Taylor and Anand, 2004; Kaminsky et al., 2009; Klein-BenDavid et al., 2009). Evidence for carbonatitic activity in the mantle is limited by volcanic sampling; however, it is noted from localities worldwide (e.g., see above references).

We document a single crystal inclusion of aragonite within olivine (Fig. 1) from Calatrava, Spain, an area where carbonatitic volcanism with mantle debris was previously reported (Bailey et al., 2005). Confirmation of the aragonite crystal structure was performed by micro-X-ray diffraction (XRD) (Fig. 2; GSA Data Repository[1]). Aragonite is stable at mantle pressures and temperatures either as a high-pressure polymorph of calcite (Redfern et al., 1989, and references therein), or by the breakdown reaction dolomite = aragonite + magnesite (Buob et al., 2006, and references therein). The aragonite stability field intersects the CO_2 + H_2O-bearing mantle solidus at ~100 km depth, providing a minimum depth for mantle crystallization. The presence of aragonite, and evidence for calcite after aragonite in other inclusions, points to a deep sublithospheric mantle source for volcanism in Calatrava.

FIELD EVIDENCE, PETROGRAPHY, AND MINERAL CHEMISTRY

Calatrava is 150 km south of Madrid in central Spain. The samples used in this study are from Moron de Villa Mayor, a leucitite volcano in the southwest of Calatrava (38°49′05.9″N, 04°07′22.4″W); it is the earliest example of volcanism in the province at 8.8–8.6 Ma (Ancochea et al., 1979). Volcanism erupted through Hercynian basement quartzite.

Villa Mayor is predominantly composed of leucitite lava, but carbonatitic activity is recorded by carbonatitic inclusions and xenoliths in the lava. The major stage of extrusion is leucitite

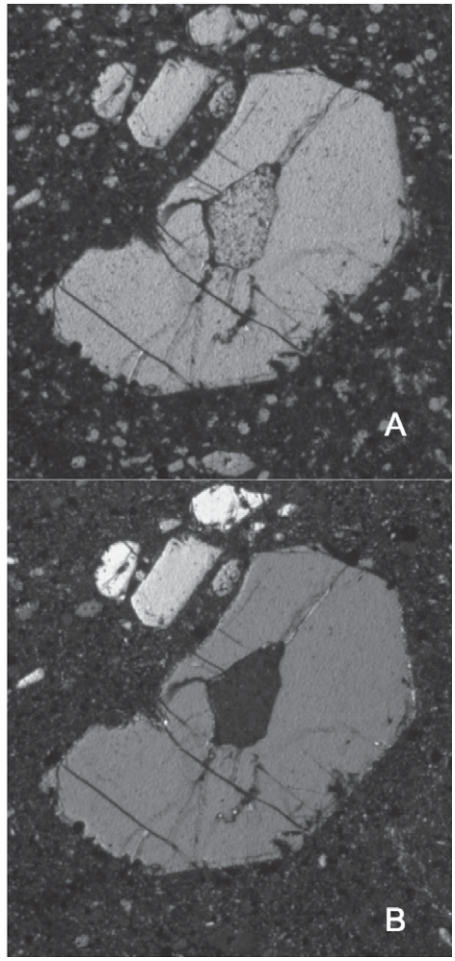

Figure 1. A: Plane polarized light photograph of olivine with aragonite inclusion. Shards of xenocrystic olivine are visible in leucitite groundmass. B: Cross-polarized light showing single aragonite crystal in full extinction. Horizontal field of view is 3 mm.

[1]GSA Data Repository item 2010253, Figures DR1–DR4, is available online at www.geosociety.org/pubs/ft2010.htm, or on request from editing@geosociety.org or Documents Secretary, GSA, P.O. Box 9140, Boulder, CO 80301, USA.

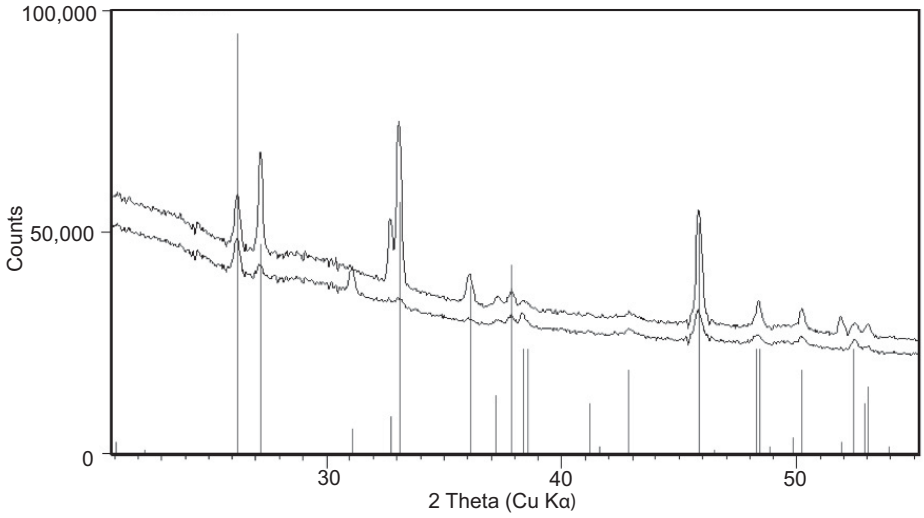

Figure 2. X-ray diffraction patterns of powdered aragonite. Peak positions match with line pattern of aragonite (Joint Committee on Powder Diffraction Standards card 41–1475). Multiple lines represent sequential analysis of same sample after powder rearrangement.

lava with olivine xenocrysts and mantle xenoliths (lherzolite and wehrlite). Olivines from this flow are the focus of this study. Almost all samples have been dry polished with a dry diamond powder, to preserve the alkali content of the carbonate (which was subsequently found to be <<1 wt%).

The leucitite is aphanitic and composed of diopside, leucite, phlogopite, nepheline, sodalite, apatite, and titanomagnetite. Olivines are not observed as phenocrysts. Calcite is present in coarsely crystalline, primary carbonatitic xenolith lenses, often associated with xenocrystic olivines. Carbonatite lenses are composed of polycrystalline calcite, phlogopite, nepheline, sodalite, and diopside, with minor titanomagnetite and apatite.

Olivine xenocrysts modally compose >30% of the leucitite lava. Olivine cores are Fo_{87}, whereas rims are Fo_{62}, suggestive of disequilibrium with the leucitite. Carbonatitic inclusions within olivines are prolific and ~90% of all inclusions studied (120) contain carbonate with or without silicate glass or silicate minerals. Calcite, aragonite, and dolomite are all identified from inclusions. Polymineralic inclusions contain silicate minerals coexisting with carbonate; typical silicates include diopside, nepheline, phlogopite, kataphorite, and sanidine. Chrome-rich spinels occur as monomineralic euhedral inclusions within olivine with Cr_2O_3 <48.7 wt%. Where inclusions trap fresh silicate glass, there is often associated carbonate. Glass compositions from inclusions do not correspond to the bulk rock analyses of the leucitite (López-Ruiz et al., 1993), even after recalculation to account for the xenocrystic olivine content (see Table 1).

The aragonite inclusion (Fig. 1) is ~500 × 800 µm, has a subhedral outline, and was initially recognized for its anomalous interference color, lack of cleavage and twinning, and low spectral dispersion. Further investigation using Raman spectroscopy also indicated aragonite (see the Data Repository). In cross-polarized light, the single aragonite crystal is in complete extinction (Fig. 1B). Examples of other inclusions with euhedral to subhedral outlines have so far proved to be polycrystalline calcite, perhaps resulting from aragonite inversion. Electron microprobe analysis (EMPA) of the aragonite is presented in Table 1. The single aragonite crystal is associated with minor phlogopite, diopside, and apatite, which were found to result from the interaction of the host leucitite lava and the aragonite crystal along a fracture. Other examples from this lava flow where lava has interacted with inclusions have resulted in embayments and extensive dissolution of the olivine grain. We thus conclude that there was minimal interaction of the aragonite with the host lava and infer that fracturing of the host olivine, in this case, occurred just prior to eruption.

ARAGONITE IDENTIFICATION BY MICRO-XRD

For analysis by XRD the sample was powdered directly from the thin section by scratching a small area from the inclusion. The high brightness X-ray source at the Natural History Museum, London, allows for characterization of microsamples without the need of a synchrotron emission source. The microdiffraction system is equipped with a GeniX Cu high flux X-ray system and a FOX 2D 10_30P mirror that delivers a 230 µm beam of copper K alpha radiation. Operating conditions of the X-ray source were 50 kV and 1 mA. The beam footprint on the sample was 230 × 800 µm. Rapid data acquisition was

TABLE 1. ELECTRON MICROPROBE ANALYSES FOR ARAGONITE, OLIVINE XENOCRYST, AND CARBONATE-BEARING GLASS INCLUSIONS, AND BULK ROCK DATA FOR LEUCITITE LAVA

	Aragonite† (n = 4)	Leucitite (López-Ruiz et al., 1993, n = 5)	Olivine§ (n = 92)	Leucitite (recalculated minus 30% olivine)	Silicate glass† (n = 4)
SiO_2	bd	44.73	40.25	46.65	55.46 (52.94–57.12)
TiO_2		2.04	bd	2.91	bd
Al_2O_3		9.53	0.07	13.58	17.70 (15.71–19.9)
Fe_2O_3		4.68		6.69	
FeO*	bd	5.50	11.88	2.77	0.23 (0.05–0.33)
MnO	bd	0.15	0.16	0.15	bd
MgO	bd	14.47	47.03	0.52	2.00 (1.64–2.56)
CaO	56.26	10.68	0.16	15.19	5.13 (4.72–6.04)
Na_2O	bd	2.17	bd	3.10	bd
K_2O	bd	3.23	bd	4.61	3.87 (3.58–4.08)
P_2O_5	0.03	0.90	bd	1.29	bd
SrO	0.18				bd
l.o.i.		1.55		2.21	
Total	56.51	99.63	99.97	99.14	84.39 (81.02–87.13)

Note: Bulk rock data are recalculated based on xenocrystic olivine content, ~30%. Glass inclusions show no evidence for alteration or devitrification; therefore low totals may reflect the volatile content of the glass. Range of analyzed values given in parentheses. Electron microprobe analysis at University of Bristol using a Cameca SX100 microprobe operating at 15 kV, 10 nA, and 5 µm beam; 20 kV, 10 nA, and1 µm beam; and 15kV, 2nA, and 5 µm beam for aragonite, olivine, and glass, respectively. All analyses used a PAP matrix correction and secondary silicate, carbonate, oxide, and glass standards. l.o.i.—loss on ignition.

*Iron measured as FeO by microprobe analysis.

†BaO, F, and Cl were analyzed but were found to be below detection limit (F—0.8 wt% and Cl—0.06 wt%). bd—concentration below microprobe detection limits. n—number of analyses.

§Olivine has Cr_2O_3 (0.05) and NiO (0.32).

achieved by using an INEL (Instrumentation Electronique) 120º curved position sensitive detector (PSD). NIST (National Institute of Standards and Technology, USA) silicon powder SRM 640 and silver behenate were used as calibration standards. The 2-theta linearization of the PSD was performed using a least-squares cubic spline function. Powdered aragonite was collected into the center of a zero-background sapphire disk. The sample was rotated during the measurements with runs lasting between 20 and 23 h.

Figure 2 details the XRD patterns obtained for the powdered inclusion. Peak positions match very well with aragonite data from the ICDD (International Centre for Diffraction Data) Powder Diffraction File, JCPDS (Joint Committee on Powder Diffraction Standards) card 41–1475. Peak intensities deviate to some degree, and a few aragonite peaks are missing as a result of a nonrandom particle distribution. The number of particles in our microsample is too small to create a uniform distribution of all possible crystallite orientations. Every rearrangement of the powder will produce different particle distributions that contribute to varying peak intensities. This is shown in Figure 2 for a repeated micro-XRD run after rearrangement of the powder, which gives a similar XRD pattern with matching peak positions, but differing peak intensities.

DISCUSSION AND IMPLICATIONS

Aragonite together with calcite and dolomite inclusions in olivine is illustrative of the carbonatitic activity in the mantle beneath Calatrava. Carbonatitic activity in Calatrava is also documented from pyroclastic deposits (Bailey et al., 2005) and mantle xenoliths (Humphreys et al., 2008). The range of carbonate inclusion compositions from Villa Mayor may reflect sustained crystallization of olivine during ascent, trapping different compositions at different depths or trapping a highly heterogeneous (immiscible?) source melt at sublithospheric depths. Pseudomorphs of calcite after aragonite are indicative of high-pressure crystallization, and disequilibrium of olivine in the leucitite melt also suggests against continued crystallization.

Aragonite is a high-pressure mineral phase in the mantle, as demonstrated from the available experimental data (Fig. 3; Irving and Wyllie, 1973; Buob et al., 2006). Petrographically the aragonite inclusion shows a subhedral crystal form within olivine, suggestive of cotectic crystallization of olivine and aragonite and resulting from the competing growth of the two phases. A preexisting aragonite crystal included in olivine would be more likely to exhibit a euhedral crystal form or a fragmentary shape. Examples of carbonate-bearing melt inclusions also indicate the activity of a carbonate-rich melt during olivine growth.

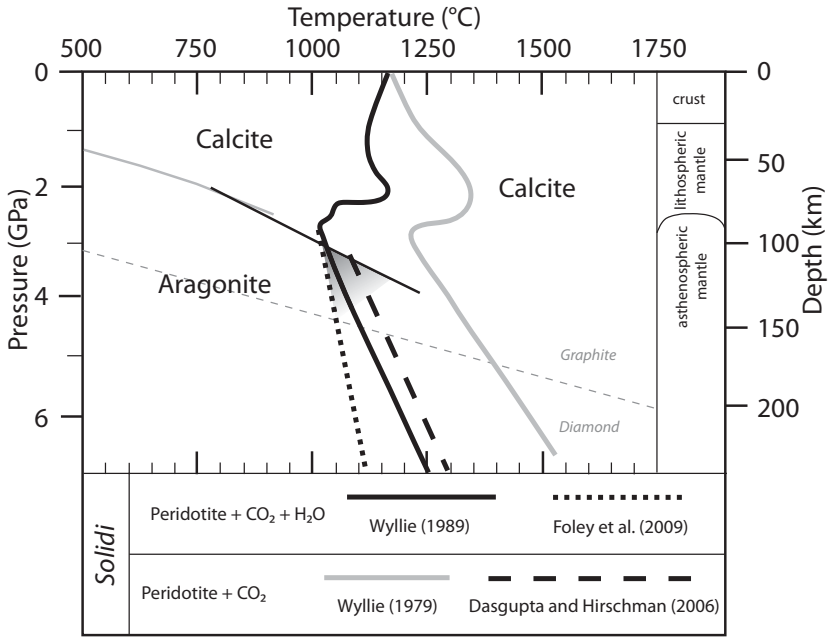

Figure 3. Pressure and temperature plot for the stability of calcium carbonate (thin lines; light gray—Redfern et al., 1989; black—Irving and Wyllie, 1973) and mantle solidi (thick lines). Shaded region indicates where aragonite may crystallize from mantle melt at 100 km and 120 km for H_2O-bearing and H_2O-absent conditions, respectively. Lithospheric cross section for Calatrava according to data from López-Ruiz et al. (1993). Graphite-diamond inversion is from Wyllie (1989).

The lithospheric thickness under Calatrava is estimated geophysically to be ~80 km (López-Ruiz et al., 1993). Using the experimentally determined solidus curves for peridotite + CO_2 + H_2O (Wyllie, 1989) and peridotite + CO_2 (Dasgupta and Hirschman, 2006), and the experimental constraints on the stability of aragonite (Irving and Wyllie, 1973), a minimum depth for the olivine xenocrysts is estimated to be between 100 and 120 km (Fig. 3). Entrainment of olivine xenocrysts indicates a source depth for leucitite melts >100–120 km.

Rapid ascent from the mantle and quenching are required to preserve the aragonite crystal structure without inversion to calcite. Rapid quenching of the melt is indicated by the microcrystalline groundmass (see Fig. 1), and the presence of glassy, carbonate-silicate melt inclusions (see the Data Repository). A rapid eruption rate is also required to transport the abundant dense xenolithic and xenocrystic (~30%) content of the lava. Diffusion of hydrogen in olivine from mantle xenoliths has illustrated the rapid exhumation rate of alkali basalts, similar to that of kimberlites at 6 ± 3 m/s (Demouchy et al., 2006). High ascent rates combined with >30% xenolithic load require an extremely high volatile content in the initial melt.

The depth constraints indicated by the presence of aragonite (and dolomite) have important implications for volcanism in Calatrava. Dependent on the presence or absence of water, the minimum depth of aragonite crystallization occurs between 100 and 120 km (Fig. 3). The depth of melt formation and then explosive ascent is thus below the depth of the geophysical lithosphere, in the sublithospheric mantle. Radiogenic lead isotope data for the inclusions and the whole rock are summarized in Figure 4, and show high $^{207}Pb/^{204}Pb$ ratios relative to both mid-oceanic ridge basalt (MORB) and ocean island basalt (OIB). Thus, the melt is unlikely to have sampled convecting asthenospheric mantle, which isotopically should be more similar to MORB and dominant OIB compositions. Rather, the carbonate inclusions have $^{207}Pb/^{204}Pb$-$^{206}Pb/^{204}Pb$ compositions similar to those of carbonate-bearing diamond inclusions (Klein-BenDavid et al., 2010; Fig. 4), corroborating their sublithospheric mantle origin. We therefore suggest that melting sampled the relatively rigid, accreted sublithospheric mantle beneath Spain. This segment of mantle presumably had a density similar to that of the convecting asthenosphere, but acted as a nonconvecting reservoir for incompatible elements, volatiles, and small-fraction partial melts.

Carbonatitic activity in the sublithospheric mantle in Spain is clearly demonstrated by our finding of aragonite, dolomite, and calcite inclusions in olivine. The presence of aragonite accords with experimental evidence and geological examples from diamond inclusions for the stability and storage of high-pressure carbonates in the deep mantle. Xenocrystic olivine indicates that the origin of the leucitite melt is

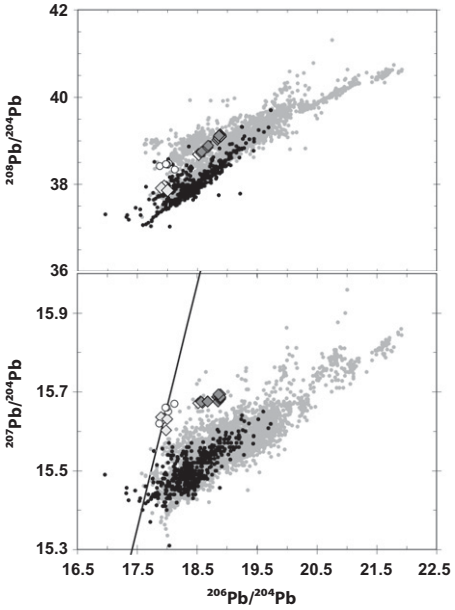

Figure 4. $^{208}Pb/^{204}Pb$ versus $^{206}Pb/^{204}Pb$ and $^{207}Pb/^{204}Pb$ versus $^{206}Pb/^{204}Pb$ plots for bulk rock samples (dark gray diamonds) and carbonate inclusions (light gray diamonds) from our own data. Mid-oceanic ridge basalt (black dots) and ocean island basalt (gray dots) are plotted for comparison (data modified from http://georoc.mpch-mainz.gwdg.de/georoc/). Diamond inclusion data (open circles) are from Klein-BenDavid et al. (2010), and geochron is plotted for reference (black line).

even deeper within the mantle and strengthens arguments for a sublithospheric mantle origin for alkaline ultramafic magmas and extrusive carbonatites.

ACKNOWLEDGMENTS

Humphreys thanks R. Avanzinelli, G. Cressey, J. Darling, J. Schumacher, F. Stoppa, G. Rosatelli, M. Walter, and A. Woolley for helpful discussions. We thank two anonymous reviewers and F.V. Kaminsky for insightful and constructive reviews. This research is funded by a NERC (Natural Environment Research Council) CASE (Co-operative Awards in Science & Engineering) Ph.D. studentship.

REFERENCES CITED

Ancochea, E., Giuliani, A., and Villa, I., 1979, Edades radiometricas K-Ar del vulcanismo de la region central esapnola: Estudios Geologica, v. 35, p. 131–135.

Bailey, D.K., 1989, Carbonate melt from the mantle in the volcanoes of southeast Zambia: Nature, v. 338, p. 415–418, doi: 10.1038/338415a0.

Bailey, D.K., 1993, Carbonate magmas: Geological Society of London Journal, v. 150, p. 637–651, doi: 10.1144/gsjgs.150.4.0637.

Bailey, D.K., and Collier, J.D., 2000, Carbonatite-melilitite association in the Italian collision zone and the Ugandan rifted craton: Significant common factors: Mineralogical Magazine, v. 64, p. 675–682, doi: 10.1180/002646100549698.

Bailey, K., Garson, M., Kearns, S., and Velasco, A.P., 2005, Carbonate volcanism in Calatrava, central Spain: A report on the initial findings: Mineralogical Magazine, v. 69, p. 907–915, doi: 10.1180/0026461056960298.

Bailey, K., Kearns, S., Mergoil, J., Daniel, J.M., and Paterson, B., 2006, Extensive dolomitic volcanism through the Limagne basin, central France: A new form of carbonatite activity: Mineralogical Magazine, v. 70, p. 231–236, doi: 10.1180/0026461067020327.

Barker, D.S., and Nixon, P.H., 1989, High-Ca, low-alkali carbonatite volcanism at Fort Portal, Uganda: Contributions to Mineralogy and Petrology, v. 103, p. 166–177, doi: 10.1007/BF00378502.

Bell, K., and Simonetti, A., 2010, Source of parental melts to carbonatites—Critical isotopic constraints: Mineralogy and Petrology, v. 98, p. 77–89, doi: 10.1007/s00710-009-0059-0.

Buob, A., Luth, B., Schmidt, M., and Ulmer, P., 2006, Experiments on $CaCO_3$-$MgCO_3$ solid solutions at high pressure and temperature: American Mineralogist, v. 91, p. 435–440, doi: 10.2138/am.2006.1910.

Coltorti, M., Bonadiman, C., Hinton, R.W., Siena, F., and Upton, B.G.J., 1999, Carbonatite metasomatism of the oceanic upper mantle: Evidence from clinopyroxenes and glasses in ultramafic xenoliths of Grande Comore, Indian Ocean: Journal of Petrology, v. 40, p. 133–165, doi: 10.1093/petrology/40.1.133.

Dasgupta, R., and Hirschman, M.M., 2006, Melting in the Earth's deep upper mantle caused by carbon dioxide: Nature, v. 440, p. 659–662, doi: 10.1038/nature04612.

Dawson, J.B., 1962, Sodium carbonate lavas from Oldoinyo Lengai, Tanganyika: Nature, v. 195, p. 1075–1076, doi: 10.1038/1951075a0.

Deines, P., and Gold, D.P., 1973, The isotopic composition of carbonatite and kimberlite carbonates and their bearing on the isotopic composition of deep-seated carbon: Geochimica et Cosmochimica Acta, v. 37, p. 1709–1733, doi: 10.1016/0016-7037(73)90158-0.

Demouchy, S., Jacobsen, S.D., Galliard, F., and Stern, C.R., 2006, Rapid magma ascent recorded by water diffusion profiles in mantle olivine: Geology, v. 34, p. 429–432, doi: 10.1130/G22386.1.

Foley, S.F., Yaxley, G.M., Rosenthal, A., Buhre, S., Kiseva, E.S., Rapp, R.P., and Jacob, D.E., 2009, The composition of near-solidus melts of peridotite in the presence of CO_2 and H_2O between 40 and 60 kbar: Lithos, v. 112, p. 274–283, doi: 10.1016/j.lithos.2009.03.020.

Humphreys, E.R., Bailey, K., Hawkesworth, C.J., Wall, F., and Hammond, S., 2008, Mantle xenoliths from the Calatrava volcanic province, Spain—Evidence for carbonatite-silicate interaction in the upper mantle: Eos (Transactions, American Geophysical Union), v. 89, fall meeting supplement, abs. V43F–2200.

Irving, A.J., and Wyllie, P.J., 1973, Melting relationships in CaO-CO_2 and MgO-CO_2 to 36 kilobars with comments on CO_2 in the mantle: Earth and Planetary Science Letters, v. 20, p. 220–225, doi: 10.1016/0012-821X(73)90161-1.

Kaminsky, F., Wirth, R., Matsyuk, S., Schreiber, A., and Thomas, R., 2009, Nyerereite and nahcolite inclusions in diamond: Evidence for lower-mantle carbonatitic magmas: Mineralogical Magazine, v. 73, p. 797–816, doi: 10.1180/minmag.2009.073.5.797.

Keller, J., 1981, Carbonatitic volcanism in the Kaiserstuhl alkaline complex: Evidence for highly fluid carbonatitic melts at the earth's surface: Journal of Volcanology and Geothermal Research, v. 9, p. 423–431, doi: 10.1016/0377-0273(81)90048-2.

Klein-BenDavid, O., Logvinova, A.M., Schrauder, M., Spetius, Z.V., Weiss, Y., Hauri, E.H., Kaminsky, F.V., Sobolev, N.V., and Navon, O., 2009, High-Mg carbonatitic microinclusions in some Yakutian diamonds—A new type of diamond-forming fluid: Lithos, v. 112S, p. 648–659, doi: 10.1016/j.lithos.2009.03.015.

Klein-BenDavid, O., Pearson, D.G., Nowell, G.M., Ottley, C., McNeil, J.C.R., and Cartigny, P., 2010, Mixed fluid sources involved in diamond growth constrained by Sr-Nd-Pb-C-N isotopes and trace elements: Earth and Planetary Science Letters, v. 289, p. 123–133, doi: 10.1016/j.epsl.2009.10.035.

López-Ruiz, J., Cebriá, J.M., Doblas, M., Oyarzun, R., Hoyos, M., and Martín, C., 1993, Cenozoic intra-plate volcanism related to extensional tectonics at Calatrava, central Iberia: Geological Society of London Journal, v. 150, p. 915–922, doi: 10.1144/gsjgs.150.5.0915.

Redfern, S.A.T., Salje, E., and Navrotsky, A., 1989, High-temperature enthalpy at the orientational order-disorder transition in calcite: Implications for the calcite/aragonite phase equilibrium: Contributions to Mineralogy and Petrology, v. 101, p. 479–484, doi: 10.1007/BF00372220.

Rosatelli, G., Wall, F., and Stoppa, F., 2007, Calcio-carbonatite melts and metasomatism in the mantle beneath Mt. Vulture (southern Italy): Lithos, v. 99, p. 229–248, doi: 10.1016/j.lithos.2007.05.011.

Rudnick, R.L., McDonough, W.F., and Chappell, B.W., 1993, Carbonatite metasomatism in the northern Tanzanian mantle: Petrographic and geochemical characteristics: Earth and Planetary Science Letters, v. 114, p. 463–475, doi: 10.1016/0012-821X(93)90076-L.

Taylor, L.A., and Anand, M., 2004, Diamonds: Time capsules from the Siberian mantle: Chemie der Erde, v. 64, p. 1–74, doi: 10.1016/j.chemer.2003.11.006.

Woolley, A.R., and Church, A.A., 2005, Extrusive carbonatites: A brief review: Lithos, v. 85, p. 1–14, doi: 10.1016/j.lithos.2005.03.018.

Woolley, A.R., and Kempe, D.R.C., 1989, Carbonatites: Nomenclature, average chemical compositions and element distribution, *in* Bell, K., ed., Carbonatites. Genesis and evolution: London, Unwin Hyman, p. 1–13.

Woolley, A.R., Barr, M.W.C., Din, V.K., Jones, G.C., Wall, F., and Williams, C.T., 1991, Extrusive carbonatites from the Uyaynah Window, United Arab Emirates: Journal of Petrology, v. 32, p. 1143–1167.

Wyllie, P.J., 1978, Mantle fluid compositions buffered in peridotite-CO_2-H_2O by carbonates, amphibole and phlogopite: Journal of Geology, v. 86, p. 687–713, doi: 10.1086/649737.

Wyllie, P.J., 1979, Petrogenesis and the physics of the Earth, *in* Yoder, H.S., Jr., ed., The evolution of the igneous rocks. Fiftieth anniversary perspectives: Princeton, New Jersey, Princeton University Press, p. 483–520.

Wyllie, P.J., 1989, Origin of carbonatites: Evidence from phase equilibrium studies, *in* Bell, K., ed., Carbonatites. Genesis and evolution: London, Unwin Hyman, p. 500–545.

Yaxley, G.M., Green, D.H., and Kamenetsky, V., 1998, Carbonatite metasomatism in the southeastern Australian lithosphere: Journal of Petrology, v. 39, p. 1917–1930, doi: 10.1093/petrology/39.11.1917.

Manuscript received 9 March 2010
Revised manuscript received 7 May 2010
Manuscript accepted 20 May 2010

Printed in USA